Bounds on Time Delay and Doppler Estimation with Partially Coherent Signals

Richard J. Kozick
Bucknell University
Electrical Engineering Dept.
Lewisburg, PA 17837
kozick@bucknell.edu

Brian M. Sadler
Army Research Laboratory
2800 Powder Mill Road
Adelphi, MD 20783
bsadler@arl.army.mil

Abstract — **Fundamental performance limits for passive time delay and Doppler estimation have been studied extensively for several decades. The fundamental limits are usually parameterized in terms of the signal-to-noise ratio (SNR) at each sensor, the spectral support of the signals (fractional bandwidth), and the time-bandwidth product of the observations. In some applications, loss of coherence between the signals measured at a pair of sensors significantly affects the time delay and Doppler estimation accuracy. For example, in aeroacoustics (low frequency sounds $<$ 300 Hz propagating through air) and ultrasonics (sounds in the MHz range propagating through living tissue), the signals received at spatially-separated sensors are not perfectly coherent due to random motion of particles in the propagation medium. In order to quantify the effect of partial signal coherence on time delay and Doppler estimation, we present Cramér-Rao and Ziv-Zakai bounds that are explicitly parameterized by the signal coherence, along with the traditional parameters of SNR, fractional bandwidth, and time-bandwidth product. The results are applied to the processing data from an "array of arrays" that consists of several small-aperture sensor arrays distributed over a large two-dimensional area.**

I. Introduction

An "array of arrays" is a collection of small-aperture sensor arrays that are distributed over a large two-dimensional area. Our objective is to use an array of arrays to estimate the location of a non-moving vehicle or track the path of a moving vehicle. An algorithm for source localization that achieves nearly optimal performance while performing local the processing at each array and limiting the communication bandwidth between the arrays and a fusion center works as follows [1, 2]. Each array estimates the source bearing and transmits the bearing estimate *and* the raw data from one sensor to the fusion center. The fusion center performs time delay estimation (TDE) between array pairs, then estimates the source location by triangulating the bearing and TD estimates. This method jointly processes data from widely-separated arrays, in contrast to the more common "bearings-only" localization/tracking algorithms, e.g., [3, 4, 5, 6, 7]. In many cases, the Cramér-Rao bound (CRB) on localization accuracy for the bearing and TD triangulation method is nearly equal to the CRB for the optimal processor that uses the raw data from all sensors at the fusion center. Further, these CRBs may be significantly smaller than the CRB for bearings-only triangulation.

Accurate TD estimates are clearly required in order to achieve improved localization accuracy relative to bearings-only triangulation. We are particularly interested in aeroacoustic tracking of ground vehicles using an array of microphone arrays. Signal coherence is known to degrade with increased spatial separation for low frequency sounds (10–300 Hz) propagating through air, e.g., [8, 9]. Our study in the present paper of TD and Doppler estimation with partially coherent signals is motivated by the issues presented above. Our goal is to quantify those scenarios in which TDE is feasible, as a function of signal coherence, SNR per sensor, fractional bandwidth of the signal, and time-bandwidth product of the observed data. The basic result is that for a given SNR, fractional bandwidth, and time-bandwidth product, there exists a "threshold coherence" value that must be exceeded in order for TDE to achieve the CRB. The analysis is based on Ziv-Zakai bounds for TDE, as in [10, 11].

TD estimation with partially coherent signals is also relevant in medical ultrasound applications, e.g., [12, 13]. The medical ultrasound application is distinguished from the aeroacoustic tracking of ground vehicles in that the former is typically an *active* system while the latter is *passive.* The medical ultrasound application therefore allows much more control over the SNR and bandwidth of the signals. In passive aeroacoustics, the received signals are emitted by a vehicle and are not controllable for the purposes of TD estimation.

This paper is organized as follows. TDE for a non-moving source is considered in Section II, including the model for the sensor data as correlated Gaussian random processes, CRBs, Ziv-Zakai bound analysis leading to the threshold coherence phenomenon, and simulation examples. TD and Doppler estimation for a moving source are briefly considered in Section III, and concluding remarks are given in Section IV.

II. TDE for a Non-Moving Source

A model is formulated in this section for the discrete-time signals received by H widely-spaced sensors, with emphasis on the case of $H = 2$ sensors.[1] Consider a single non-moving source that is located at coordinates (x_s, y_s) in the (x, y) plane. The H sensors are distributed in the same plane, at coordinates (x_h, y_h), for $h = 1, \ldots, H$. If c is the speed of propagation, then the propagation time from the source to sensor h is

$$\tau_h = \frac{d_h}{c} = \frac{1}{c}\left[(x_s - x_h)^2 + (y_s - y_h)^2\right]^{1/2}, \qquad (1)$$

where d_h is the distance from the source to sensor h.

[1] In the array of arrays scenario described in Section I, the H sensors considered here are located on *distinct* arrays.

The signal received at sensor h due to the source will be represented as $s_h(t-\tau_h)$, where the signals in the vector $\mathbf{s}(t) = [s_1(t), \ldots, s_H(t)]^T$ are modeled as real-valued, continuous-time, zero-mean, jointly wide-sense stationary, Gaussian random processes with $-\infty < t < \infty$. These processes are fully specified by the $H \times H$ cross-correlation function matrix

$$\mathbf{R}_s(\tau) = E\{\mathbf{s}(t+\tau)\,\mathbf{s}(t)^T\}, \tag{2}$$

where E denotes expectation, superscript T denotes transpose, and we will later use the notation superscript $*$ and superscript H to denote complex conjugate and conjugate transpose, respectively. The (g,h) element in (2) is the cross-correlation function

$$r_{s,gh}(\tau) = E\{s_g(t+\tau)\,s_h(t)\} \tag{3}$$

between the signals received at sensors g and h. The correlation functions (2) and (3) are equivalently characterized by their Fourier transforms, which are the cross-spectral density functions

$$G_{s,gh}(\omega) = \mathcal{F}\{r_{s,gh}(\tau)\} = \int_{-\infty}^{\infty} r_{s,gh}(\tau)\exp(-j\omega\tau)\,d\tau \tag{4}$$

and the associated cross-spectral density matrix

$$\mathbf{G}_s(\omega) = \mathcal{F}\{\mathbf{R}_s(\tau)\}. \tag{5}$$

The diagonal elements $G_{s,hh}(\omega)$ of (5) are the power spectral density (PSD) functions of the signals $s_h(t)$, and hence they describe the distribution of average signal power with frequency. The model allows the PSD to vary from one sensor to another to reflect propagation differences and source aspect angle differences.

The off-diagonal elements of (5), $G_{s,gh}(\omega)$, are the cross-spectral density (CSD) functions for the signals $s_g(t)$ and $s_h(t)$ received at distinct sensors $g \neq h$. In general, the CSD functions have the form

$$G_{s,gh}(\omega) = \gamma_{s,gh}(\omega)\;[G_{s,gg}(\omega)G_{s,hh}(\omega)]^{1/2}, \tag{6}$$

where $\gamma_{s,gh}(\omega)$ is the *spectral coherence function* for the signals, which has the property $0 \le |\gamma_{s,gh}(\omega)| \le 1$. Coherence magnitude $|\gamma_{s,gh}(\omega)| = 1$ corresponds to perfect correlation between the signals at sensors g and h, while the partially coherent case $|\gamma_{s,gh}(\omega)| < 1$ models random effects in the propagation paths from the source to sensors g and h.

The observed signal at sensor h is modeled as a sum of the delayed source signal and noise,

$$z_h(t) = s_h(t-\tau_h) + w_h(t), \tag{7}$$

where the noise signals $w_h(t)$ are modeled as real-valued, continuous-time, zero-mean, jointly wide-sense stationary, Gaussian random processes that are mutually uncorrelated at distinct sensors, and are uncorrelated from the signals. That is, the noise correlation properties are

$$\begin{aligned} E\{w_g(t+\tau)w_h(t)\} &= r_w(\tau)\,\delta_{gh} \quad (8)\\ E\{w_g(t+\tau)s_h(t)\} &= 0, \quad (9)\end{aligned}$$

where $r_w(\tau)$ is the noise autocorrelation function, and the noise PSD is $G_w(\omega) = \mathcal{F}\{r_w(\tau)\}$. We then collect the observations from the H sensors into a vector

$$\mathbf{Z}(t) = \begin{bmatrix} z_1(t) \\ \vdots \\ z_H(t) \end{bmatrix}. \tag{10}$$

The elements of $\mathbf{Z}(t)$ in (10) are zero-mean, jointly wide-sense stationary, Gaussian random processes. The CSD matrix of $\mathbf{Z}(t)$ has the form

$$\mathbf{G_Z}(\omega) = G_w(\omega)\,\mathbf{I} + \begin{bmatrix} G_{s,11}(\omega) & \cdots & e^{-j\omega D_{1H}}G_{s,1H}(\omega) \\ \vdots & \ddots & \vdots \\ e^{+j\omega D_{1H}}G_{s,1H}(\omega)^* & \cdots & G_{s,HH}(\omega) \end{bmatrix}, \tag{11}$$

where the relative time delay of the signal at sensors g,h is

$$D_{gh} = \tau_g - \tau_h. \tag{12}$$

For $H = 2$ sensors, if we define $D = D_{21} = \tau_2 - \tau_1$, the CSD matrix in (11) has the form

$$\begin{aligned}\mathrm{CSD}\begin{bmatrix} z_1(t) \\ z_2(t)\end{bmatrix} &= \mathbf{G_Z}(\omega) \quad (13)\\ &= \begin{bmatrix} G_{s,11}(\omega)+G_w(\omega) & e^{+j\omega D}\,G_{s,12}(\omega) \\ e^{-j\omega D}\,G_{s,12}(\omega)^* & G_{s,22}(\omega)+G_w(\omega)\end{bmatrix},\end{aligned}$$

where the CSD $G_{s,12}(\omega)$ in (13) can be expressed in terms of the signal spectral coherence $\gamma_{s,12}(\omega)$ using (6):

$$G_{s,12}(\omega) = \gamma_{s,12}(\omega)\;[G_{s,11}(\omega)\,G_{s,22}(\omega)]^{1/2}. \tag{14}$$

The signal coherence function $\gamma_{s,12}(\omega)$ describes the degree of correlation that remains in the signal emitted by the source at each frequency ω after propagating to sensors 1 and 2. Next, we develop an SNR-like expression for the two-sensor case that appears in all subsequent expressions for fundamental limits on TD and Doppler estimation. We begin with the magnitude-squared coherence (MSC) of the observed signals $z_1(t), z_2(t)$ as a function of the signal coherence magnitude, $|\gamma_{s,12}(\omega)|$, and other spectral density parameters:

$$\begin{aligned}\mathrm{MSC}_z\left(|\gamma_{s,12}(\omega)|\right) &= \frac{|\mathrm{CSD}[z_1(t),z_2(t)]|^2}{\mathrm{PSD}[z_1(t)]\cdot\mathrm{PSD}[z_2(t)]}\\ &= \frac{|\gamma_{s,12}(\omega)|^2\;G_{s,11}(\omega)G_{s,22}(\omega)}{[G_{s,11}(\omega)+G_w(\omega)]\;[G_{s,22}(\omega)+G_w(\omega)]}\\ &= \frac{|\gamma_{s,12}(\omega)|^2}{\left[1+\left(\frac{G_{s,11}(\omega)}{G_w(\omega)}\right)^{-1}\right]\left[1+\left(\frac{G_{s,22}(\omega)}{G_w(\omega)}\right)^{-1}\right]} \quad (15)\\ &\le 1\end{aligned}$$

Then the following "SNR" expression appears in subsequent performance bounds:

$$\begin{aligned}\mathrm{SNR}\left(|\gamma_{s,12}(\omega)|\right) &= \frac{\mathrm{MSC}_z\left(|\gamma_{s,12}(\omega)|\right)}{1-\mathrm{MSC}_z\left(|\gamma_{s,12}(\omega)|\right)} \quad (16)\\ &= \left\{\frac{1}{|\gamma_{s,12}(\omega)|^2}\left[1+\left(\frac{G_{s,11}(\omega)}{G_w(\omega)}\right)^{-1}\right]\cdot\right.\\ &\qquad \left.\left[1+\left(\frac{G_{s,22}(\omega)}{G_w(\omega)}\right)^{-1}\right]-1\right\}^{-1} \quad (17)\\ &\le \frac{|\gamma_{s,12}(\omega)|^2}{1-|\gamma_{s,12}(\omega)|^2}. \quad (18)\end{aligned}$$

The inequality (18) shows that signal coherence loss ($|\gamma_{s,12}(\omega)| < 1$) severely limits the "SNR" quantity that characterizes performance, even if the SNR per sensor $G_{s,ii}(\omega)/G_w(\omega)$ is very large.

A CRB for TDE

The Cramér-Rao bound (CRB) provides a lower bound on the variance of any unbiased estimator. The problem of interest is estimation of the relative time delay vector $\mathbf{\Theta} = [D_{21}, \ldots, D_{H1}]^T$ using T samples of the sensor signals $\mathbf{Z}(0), \mathbf{Z}(T_s), \ldots, \mathbf{Z}((T-1)\cdot T_s)$, where T_s is the sampling period. The total observation time is $\mathcal{T} = T \cdot T_s$. Let us denote the sampling rate by $f_s = 1/T_s$ and $\omega_s = 2\pi f_s$. We will assume that the continuous-time random processes $\mathbf{Z}(t)$ are band-limited, and that the sampling rate f_s is greater than twice the bandwidth of the processes. Then Friedlander [14, 15] has shown that the Fisher information matrix (FIM) $\mathbf{J}$ for the parameters $\mathbf{\Theta}$ based on the samples $\mathbf{Z}(0), \mathbf{Z}(T_s), \ldots, \mathbf{Z}((T-1)\cdot T_s)$ has elements

$$J_{ij} = \frac{\mathcal{T}}{4\pi} \int_0^{\omega_s} \mathrm{tr}\left\{ \frac{\partial\, \mathbf{G_Z}(\omega)}{\partial\, \theta_i}\, \mathbf{G_Z}(\omega)^{-1} \frac{\partial\, \mathbf{G_Z}(\omega)}{\partial\, \theta_j}\, \mathbf{G_Z}(\omega)^{-1} \right\} d\omega, \tag{19}$$

where "tr" denotes the trace of the matrix. The CRB matrix $\mathbf{C} = \mathbf{J}^{-1}$ then has the property that the covariance matrix of any unbiased estimator $\hat{\mathbf{\Theta}}$ satisfies $\mathrm{Cov}(\hat{\mathbf{\Theta}}) - \mathbf{C} \geq \mathbf{0}$, where $\geq \mathbf{0}$ means that $\mathrm{Cov}(\hat{\mathbf{\Theta}}) - \mathbf{C}$ is positive semidefinite [16]. Equation (19) provides a convenient way to compute the FIM for TDE as a function of the signal coherence between sensors, the signal and noise bandwidth and power spectra, and the sensor placement geometry. We used a similar approach to evaluate the CRB for source localization in the array of arrays context in [1, 2].

We can use (13), (14), and (19) to find the CRB for TDE with $H = 2$ sensors, yielding

$$\mathrm{CRB}(D) = \frac{4\pi}{\mathcal{T}} \left[\int_0^{\omega_s} \omega^2\, \mathrm{SNR}\left(|\gamma_{s,12}(\omega)|\right)\, d\omega \right]^{-1}, \tag{20}$$

where $\mathcal{T}$ is the total observation time of the sensor data and $\mathrm{SNR}\left(|\gamma_{s,12}(\omega)|\right)$ is defined in (17). Let us consider the case in which the signal PSDs, the noise PSD, and the coherence are flat (constant) over a bandwidth $\Delta\omega$ rad/sec centered at ω_0 rad/sec. If we omit the frequency dependence of $G_{s,11}, G_{s,22}, G_w$, and $\gamma_{s,12}$, then the integral in (20) may be evaluated to yield the CRB expressions in (21), (22), and (23) in Figure 1. The quantity $\left(\frac{\Delta\omega\cdot\mathcal{T}}{2\pi}\right)$ is the time-bandwidth product of the observations, $\left(\frac{\Delta\omega}{\omega_0}\right)$ is the fractional bandwidth of the signal, and $G_{s,hh}/G_w$ is the SNR at sensor h. The CRB in (22) agrees with known results for perfectly coherent signals, e.g., [17], and with results from the ultrasonics literature [12, 13] for partially correlated speckle signals. Note from the high-SNR limit in (23) that when the signals are partially coherent $|\gamma_{s,12}| < 1$, increased source power does not reduce the CRB. Improved TDE accuracy is obtained with partially coherent signals by increasing the observation time $\mathcal{T}$ or changing the spectral support of the signal, which is $[\omega_0 - \Delta\omega/2, \omega_0 + \Delta\omega/2]$. The spectral support of the signal is not controllable in passive TDE applications, so increased observation time is the only means for improving the TDE accuracy with partially coherent signals. Source motion becomes more important during long observation times, and in Section III we extend the model to include source motion.

B Ziv-Zakai bounds for TDE

With perfectly coherent signals, it is well-known that the CRB on TDE is achievable only when the SNR expression in (17) (with $|\gamma_{s,12}(\omega)| = 1$) exceeds a threshold [10, 11]. Next we show that for TDE with partially coherent signals, a similar threshold phenomenon occurs with respect to *coherence*. That is, the coherence must exceed a threshold in order to achieve the CRB (20) on TDE. We state the threshold coherence formula for the following simplified scenario. The signal and noise spectra are flat over a bandwidth of $\Delta\omega$ rad/sec centered at ω_0 rad/sec, and the observation time is $\mathcal{T}$ seconds. Further, assume that the signal PSDs are identical at each sensor, and define the following constants for notational simplicity:

$$G_{s,11}(\omega_0) = G_{s,22}(\omega_0) = G_s, \quad G_w(\omega_0) = G_w, \quad \text{and } \gamma_{s,12}(\omega_0) = \gamma_s. \tag{24}$$

Then the SNR expression in (17) has the form

$$\mathrm{SNR}(|\gamma_s|) = \left[\frac{1}{|\gamma_s|^2} \left(1 + \frac{1}{(G_s/G_w)}\right)^2 - 1 \right]^{-1}. \tag{25}$$

Analysis of the Ziv-Zakai bound in [10, 11] shows that the threshold SNR for CRB attainability is a function of the time-bandwidth product $\left(\frac{\Delta\omega\cdot\mathcal{T}}{2\pi}\right)$ and the fractional bandwidth $\left(\frac{\Delta\omega}{\omega_0}\right)$,

$$\mathrm{SNR_{thresh}} = \frac{6}{\pi^2 \left(\frac{\Delta\omega\mathcal{T}}{2\pi}\right)} \left(\frac{\omega_0}{\Delta\omega}\right)^2 \left[\varphi^{-1}\left(\frac{1}{24}\left(\frac{\Delta\omega}{\omega_0}\right)^2 \right) \right]^2 \tag{26}$$

where $\varphi(y) = 1/\sqrt{2\pi}\int_y^\infty \exp(-t^2/2)\, dt$. It follows that the threshold coherence value is

$$|\gamma_s|^2 \geq \frac{\left(1 + \frac{1}{(G_s/G_w)}\right)^2}{1 + \frac{1}{\mathrm{SNR_{thresh}}}}, \tag{27}$$

which for high SNR becomes

$$|\gamma_s|^2 \geq \frac{1}{1 + \frac{1}{\mathrm{SNR_{thresh}}}} \quad \text{as} \quad \frac{G_s}{G_w} \to \infty. \tag{28}$$

For a specific TDE scenario, the threshold SNR for CRB attainability is given by (26), and (27) provides a corresponding threshold coherence for CRB attainability. Since $|\gamma_s|^2 \leq 1$, (27) is useful only if $G_s/G_w > \mathrm{SNR_{thresh}}$.

Figure 2 contains plots of the threshold coherence in (27) as a function of the time-bandwidth product $\left(\frac{\Delta\omega\cdot\mathcal{T}}{2\pi}\right)$, SNR $\frac{G_s}{G_w}$, and fractional bandwidth $\left(\frac{\Delta\omega}{\omega_0}\right)$. Note that $\frac{G_s}{G_w} = 10$ dB is nearly equivalent to $\frac{G_s}{G_w} \to \infty$. We note that very large time-bandwidth product is required to overcome coherence loss when the fractional bandwidth is small at 0.1. The variation of threshold coherence with fractional bandwidth is illustrated in Figure 2d. For a fixed threshold coherence value, such as 0.7, each doubling of the fractional bandwidth reduces the required time-bandwidth product by about a factor of 10.

Let us examine a narrowband signal scenario that is typical in aeroacoustics, with center frequency $f_o = \omega_o/(2\pi) = 50$ Hz and bandwidth $\Delta f = \Delta\omega/(2\pi) = 5$ Hz, so the fractional bandwidth is $\Delta f/f_o = 0.1$. From Figure 2a, coherence $|\gamma_s| = 0.8$ requires time-bandwidth product $\Delta f \cdot \mathcal{T} > 200$, so the necessary time duration $\mathcal{T} = 40$ sec for TDE may be impractical for moving sources.

Larger time-bandwidth products of the observed signals are required in order to make TDE feasible in environments with

$$
\begin{aligned}
\mathrm{CRB}(D) &= \frac{1}{2\omega_0^2\left(\frac{\Delta\omega\,\mathcal{T}}{2\pi}\right)\left[1+\frac{1}{12}\left(\frac{\Delta\omega}{\omega_0}\right)^2\right]\mathrm{SNR}\left(|\gamma_{s,12}|\right)} && (21)\\
&= \frac{1}{2\omega_0^2\left(\frac{\Delta\omega\,\mathcal{T}}{2\pi}\right)\left[1+\frac{1}{12}\left(\frac{\Delta\omega}{\omega_0}\right)^2\right]}\left\{\frac{1}{|\gamma_{s,12}|^2}\left[1+\left(\frac{G_{s,11}}{G_w}\right)^{-1}\right]\left[1+\left(\frac{G_{s,22}}{G_w}\right)^{-1}\right]-1\right\} && (22)\\
&> \frac{1}{2\omega_0^2\left(\frac{\Delta\omega\,\mathcal{T}}{2\pi}\right)\left[1+\frac{1}{12}\left(\frac{\Delta\omega}{\omega_0}\right)^2\right]}\left[\frac{1}{|\gamma_{s,12}|^2}-1\right]. && (23)
\end{aligned}
$$

Fig. 1: Expressions for CRB on time delay D for 2 sensors.

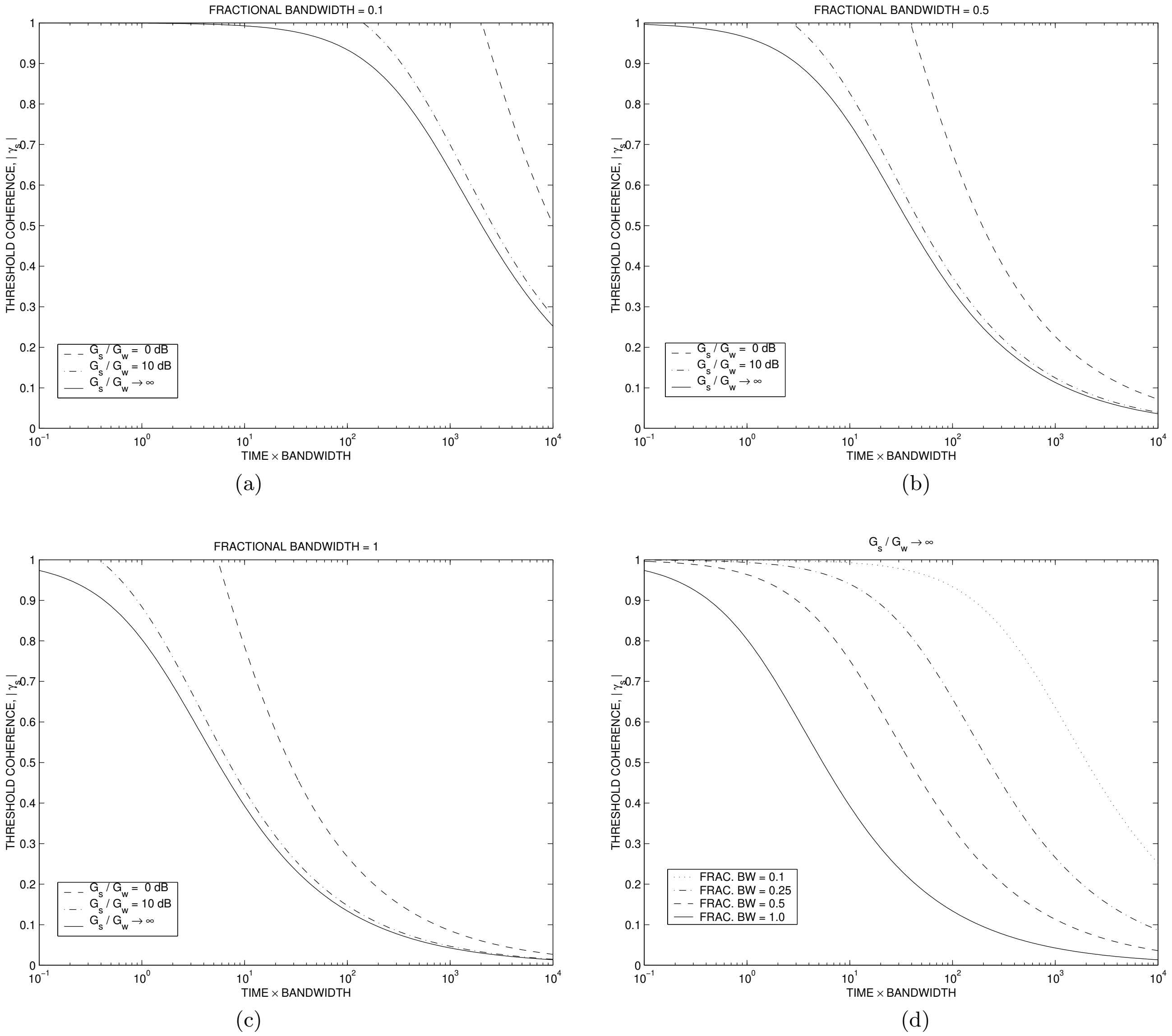

Fig. 2: Threshold coherence value from (27) versus time-bandwidth product $\left(\frac{\Delta\omega\cdot\mathcal{T}}{2\pi}\right)$ and SNR G_s/G_w for fractional bandwidth values $\left(\frac{\Delta\omega}{\omega_0}\right)$ (a) 0.1, (b) 0.5, (c) 1.0. In (d), the high SNR curves $G_s/G_w \to \infty$ are superimposed for several values of fractional bandwidth.

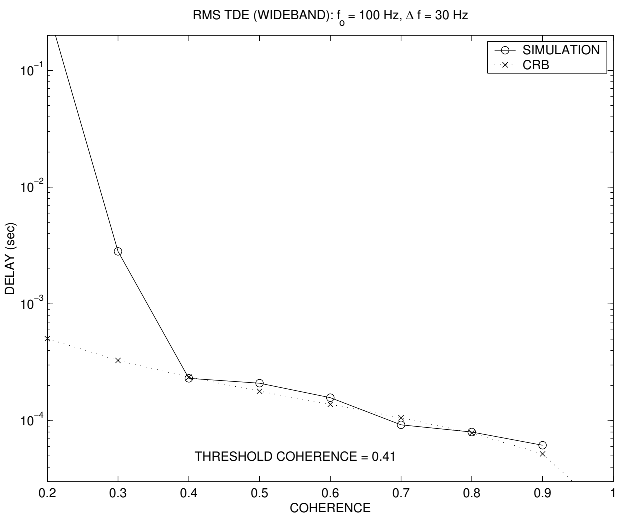

Fig. 3: Comparison of simulated RMS error for TDE with CRBs and threshold coherence value for a wideband signal with $\Delta f = 30$ Hz centered at $f_0 = 100$ Hz.

signal coherence loss. As discussed with respect to the CRB in Section II.A, only the observation time is controllable in passive applications, thus leading us to consider source motion models in Section III. The remainder of this section continues to focus on non-moving sources, with a simulation example presented in Section II.C that verifies the CRB and threshold coherence values for TDE.

C TDE simulation example

Consider TDE at $H = 2$ sensors with varying signal coherence γ_s. Our simulation example involves a signal with bandwidth $\Delta f = 30$ Hz that is centered at $f_0 = 100$ Hz, so the fractional bandwidth $\Delta f / f_0 = 0.3$. The signal, noise, and coherence are flat over the frequency band, with SNR $G_s/G_w = 100$ (20 dB). The signals and noise are band-pass Gaussian random processes. The sampling rate in the simulation is $f_s = 10^4$ samples/sec, with $T = 3 \times 10^4$ samples, so the time interval length is $\mathcal{T} = 3$ sec.

Figure 3 displays the simulated RMS error on TDE for $0.2 \le \gamma_s \le 1.0$, along with the corresponding CRB from (22) in Figure 1. The simulated RMS error is based on 100 runs, and the TDE is estimated from the location of the maximum of the cross-correlation of the sensor signals. The threshold coherence for this case is 0.41, which is calculated using (27) and (26). Note in Figure 3 that the simulated RMS error on TDE diverges sharply from the CRB very near to the threshold coherence value of 0.41, illustrating the accuracy of the analytical threshold coherence in (27).

III. Tracking a Moving Source

We have extended the non-moving source model in Section II to allow the source to move with constant velocity along a straight line. Over long observation intervals, applying the non-moving source model to a moving source leads to inaccurate localization, as quantified in [18], [19]. The source motion provides information for localization and tracking, and we have extended the CRB on differential Doppler estimation from [20] to the case of partially coherent signals. As in [20], the CRB on differential Doppler is a scalar multiple of the CRB on TDE in (20). The Ziv-Zakai considerations are not relevant to differential Doppler estimation, so there is no threshold coherence phenomenon for differential Doppler estimation.

First, we extend the non-moving source model from Section II using first-order motion models. The source position trajectory is modeled as a straight line with constant velocity over an interval of length $\mathcal{T}$,

$$x_s(t) = x_{s,0} + \dot{x}_s \cdot (t - t_0), \quad t_0 \le t \le t_0 + \mathcal{T} \tag{29}$$

$$y_s(t) = y_{s,0} + \dot{y}_s \cdot (t - t_0), \tag{30}$$

so $\dot{x}_s, \dot{y}_s$ are the velocity components. The source trajectory parameter vector is

$$\mathbf{\Theta} = [x_{s,0}, \dot{x}_s, y_{s,0}, \dot{y}_s]^T, \tag{31}$$

and the (time-varying) propagation time from the source to sensor h follows from (1),

$$\tau_h(t) = \frac{d_h(t)}{c} = \frac{1}{c}\left[(x_s(t) - x_h)^2 + (y_s(t) - y_h)^2\right]^{1/2}. \tag{32}$$

We can show that the propagation time to sensor h is approximated by

$$\tau_h(t) \approx \tau_h(t_0) + \frac{v_{r,h}(t_0)}{c} \cdot (t - t_0), \tag{33}$$

where $d_h(t_0)$ and $v_{r,h}(t_0)$ are the source range and radial velocity at the start of the time interval $t = t_0$. The approximation (33) is valid as long as the total motion during the time interval $\mathcal{T}$ is much less than the range, i.e., $|2\,\dot{x}_s\mathcal{T}| \ll d_h(t_0)$ and $|2\,\dot{y}_s\mathcal{T}| \ll d_h(t_0)$.

Next we use the approximation (33) and model the received signal at sensor h as

$$s_h\left(t - \tau_h(t)\right) \approx s_h\left(\alpha_h\, t - \tau_h(t_0) + \frac{v_{r,h}(t_0)\, t_0}{c}\right), \tag{34}$$

where

$$\alpha_h = 1 - \frac{v_{r,h}(t_0)}{c} \tag{35}$$

is the Doppler compression and

$$\tau_h(t_0) = \frac{d_h(t_0)}{c} = \frac{1}{c}\left[(x_{s,0} - x_h)^2 + (y_{s,0} - y_h)^2\right]^{1/2} \tag{36}$$

is the propagation delay at the initial time $t = t_0$. Without loss of generality, we set $t_0 = 0$, so the received signal at sensor h is

$$s_h\left(\alpha_h\, t - \tau_h(0)\right), \quad h = 1, \ldots, H, \tag{37}$$

which is the extension of the signal component of (7) to the moving source case.

The signal at each sensor, $s_h\left[\left(1 - \frac{v_{r,h}(0)}{c}\right)t - \tau_h(0)\right]$, $h = 1, \ldots, H$, is a wide-sense stationary Gaussian random process. However, for two sensors g, h with *unequal* Doppler $v_{r,g}(0) \ne v_{r,h}(0)$, the signals at sensors g, h are not *jointly* wide-sense stationary [18, 20], complicating the analytical description and the CRB performance analysis. The jointly nonstationary sensor signals generally are not characterized by a cross-spectral density matrix, so the CRB is not the inverse of a FIM of the form (19). An approximate CRB analysis for TDE with jointly nonstationary signals is given in [18]. The CRB analysis is rigorously justified in [20] and extended to CRBs on differential Doppler. A clever transformation is used in [20] so that the jointly nonstationary signals are locally modeled by a CSD of the form (11), and it is shown that the representation is accurate for CRB analysis.

We can formulate the results in [20] for the case of partially coherent signals[2], from which we make the following observations for $H = 2$ sensors. The results are valid for large observation time ($\mathcal{T}$ much larger than the coherence time of the signals and noise). The TD is $D_{12} = \tau_1(0) - \tau_2(0)$ and the differential Doppler is $\Delta v_{12} = v_{r,1}(0) - v_{r,2}(0)$.

- Estimation of TDE and differential Doppler are decoupled, so the CRB on D_{12} is given by (20), which is identical to the non-moving source case.
- The threshold coherence analysis for TDE in (27) and Figure 2 extends to the moving source case. In the ideal case that Doppler effects are perfectly estimated and compensated, the TDE problem that remains is identical to the non-moving source case. Doppler estimation is less demanding in terms of time-bandwidth product compared with TDE. Indeed, Doppler estimation is possible with sinusoidal signals that have negligible bandwidth [20].
- The CRB on differential Doppler [20], modified for partially-coherent signals, is

$$\mathrm{CRB}(\Delta v_{12}) = \frac{24\pi}{\mathcal{T}} \left(\frac{c}{\mathcal{T}}\right)^2 \left[2 \int_0^{\omega_s} \omega^2 \, \mathrm{SNR}\left(|\gamma_{s,12}(\omega)|\right) \, d\omega \right]^{-1} \quad (38)$$

  Note that (38) is a scalar multiple of the CRB on TDE in (20). The CRB on differential Doppler may be achievable in scenarios where the time-bandwidth product is insufficient for TDE.

  Interestingly, differential Doppler provides sufficient information for source localization, even without TDE, as long as five or more sensors are available [20]. Thus the source motion may be exploited in scenarios where TDE is not feasible, such as narrowband signals [20].

IV. Concluding Remarks

We have presented performance bounds for time delay and Doppler estimation when the signals received at the sensors suffer coherence loss during propagation. The results are applicable to the localization and tracking of ground vehicles with an aeroacoustic array of arrays. The bounds quantify the requirements on signal coherence, signal bandwidth, observation time, and SNR such that TDE is feasible between widely-spaced sensors. If the TDE is feasible, then improved source localization accuracy may be possible with an array of arrays compared with bearings-only triangulation. In continuing work, we have extended the two-sensor results presented here to $H > 2$ sensors, following the analysis in [21].

References

[1] R.J. Kozick and B.M. Sadler, "Source Localization with Distributed Sensor Arrays and Partial Spatial Coherence," *SPIE 2000 AeroSense Symp.*, Orlando, FL, pp. 142-153, April 24-28, 2000.

[2] R.J. Kozick and B.M. Sadler, "Distributed Source Localization with Multiple Sensor Arrays and Frequency-Selective Spatial Coherence," *Proc. 10th IEEE Workshop on Statistical Signal and Array Processing (SSAP 2000)*, Pocono Manor, PA, pp. 419-423, Aug. 14-16, 2000.

[3] R.R. Tenney and J.R. Delaney, "A distributed aeroacoustic tracking algorithm," *Proc. American Control Conf.*, pp. 1440-1450, June 1984.

[4] Y. Bar-Shalom and X.-R. Li, *Multitarget-Multisensor Tracking: Principles and Techniques*, YBS, 1995.

[5] A. Farina, "Target tracking with bearings-only measurements," *Signal Processing*, vol. 78, pp. 61-78, 1999.

[6] B. Ristic, S. Arulampalam, C. Musso, "The influence of communication bandwidth on target tracking with angle only measurements from two platforms," *Signal Processing*, vol. 81, pp. 1801-1811, 2001.

[7] L.M. Kaplan, P. Molnar, Q. Le, "Bearings-only target localization for an acoustical unattended ground sensor network," *Proc. SPIE AeroSense*, Orlando, Florida, April 2001.

[8] D.K. Wilson, "Performance bounds for acoustic direction-of-arrival arrays operating in atmospheric turbulence," *J. Acoust. Soc. Am.*, vol. 103, no. 3, pp. 1306-1319, March 1998.

[9] D.K. Wilson, "Atmospheric effects on acoustic arrays: a broad perspective from models," *1999 Meeting of the IRIS Specialty Group on Battlefield Acoustics and Seismics*, Laurel, MD, September 13-15, 1999.

[10] A.J. Weiss and E. Weinstein, "Fundamental limitations in passive time delay estimation - part 1: narrowband systems," *IEEE Trans. Acoust., Speech, Sig. Proc.*, vol. ASSP-31, no. 2, pp. 472-485, April 1983.

[11] E. Weinstein and A.J. Weiss, "Fundamental limitations in passive time delay estimation - part 2: wideband systems," *IEEE Trans. Acoust., Speech, Sig. Proc.*, vol. ASSP-32, no. 5, pp. 1064–1077, Oct. 1984.

[12] W.F. Walker and G.E. Trahey, "A fundamental limit on delay estimation using partially correlated speckle signals," *IEEE Trans. on Ultrasonics, Ferroelectrics, and Frequency Control*, vol. 42, no. 2, pp. 301–308, March 1995.

[13] I. Cespedes, J. Ophir, S.K. Alam, "The combined effect of signal decorrelation and random noise on the variance of time delay estimation," *IEEE Trans. on Ultrasonics, Ferroelectrics, and Frequency Control*, vol. 44, no. 1, pp. 220-225, Jan. 1997.

[14] B. Friedlander, "On the Cramer-Rao Bound for Time Delay and Doppler Estimation," *IEEE Trans. on Info. Theory*, vol. IT-30, no. 3, pp. 575-580, May 1984.

[15] P. Whittle, "The analysis of multiple stationary time series," *J. Royal Statist. Soc.*, vol. 15, pp. 125-139, 1953.

[16] S.M. Kay, *Fundamentals of Statistical Signal Processing: Estimation Theory*, Prentice-Hall, 1993.

[17] G.C. Carter (ed.), *Coherence and Time Delay Estimation* (Selected Reprint Volume), IEEE Press, 1993.

[18] C.H. Knapp and G.C. Carter, "Estimation of time delay in the presence of source or receiver motion," *J. Acoust. Soc. Am.*, vol. 61, no. 6, pp. 1545-1549, June 1977.

[19] W.B. Adams, J.P. Kuhn, W.P. Whyland, "Correlator compensation requirements for passive time-delay estimation with moving source or receivers," *IEEE Trans. Acoust., Speech, Signal Processing*, vol. ASSP-28, no. 2, pp. 158-168, April 1980.

[20] P.M. Schultheiss and E. Weinstein, "Estimation of differential Doppler shifts," *J. Acoust. Soc. Am.*, vol. 66, no. 5, pp. 1412-1419, Nov. 1979.

[21] E. Weinstein, "Decentralization of the Gaussian maximum likelihood estimator and its applications to passive array processing," *IEEE Trans. Acoust., Speech, Sig. Proc.*, vol. ASSP-29, no. 5, pp. 945-951, October 1981.

[2] The signal coherence between the signals at sensors g and h is defined assuming perfect compensation of the Doppler compression α_g, α_h, thus yielding the definition in (6).